A Comparative Theoretical Investigation of Three Sodalite Systems: $Cd_4S(AlO_2)_6$, $Zn_4O(BO_2)_6$, and $Zn_4S(BO_2)_6$

Maurizio Casarin,*,† Chiara Maccato,*,† and Andrea Vittadini‡

Dipartimento di Chimica Inorganica, Metallorganica ed Analitica, Università degli Studi di Padova, Padova, Italy, and Centro di Studio della Stabilità e Reattività dei Composti di Coordinazione (C.N.R.), Padova, Italy

Received: October 17, 2001; In Final Form: December 21, 2001

Periodic density functional calculations on three sodalites [$Cd_4S(AlO_2)_6$, $Zn_4O(BO_2)_6$, and $Zn_4S(BO_2)_6$] were performed. Lowest-energy allowed electronic transitions were always found to be localized on the M_4X (M = Cd, Zn; X = O, S) clusters encapsulated into lattice cages. Predicted excitation energies were only slightly affected by the adopted exchange correlation energy functional. A comparison between the optical behavior of $Cd_4S(AlO_2)_6$, $Zn_4O(BO_2)_6$, and $Zn_4S(BO_2)_6$ and that of a series of polynuclear clusters ([$Cd_4(\mu_4$-S){μ-$S_2As(CH_3)_2$}$_6$], [$Zn_4(\mu_4$-O){μ-O_2CCH_3}$_6$], [$Zn_4(\mu_4$-O){μ-O_2CNEt_2}$_6$], and [$Zn_4(\mu_4$-S){μ-$S_2P(OC_2H_5)_2$}$_6$]) indicates that only complexes with a central S atom reasonably mimic the electronic properties of the sodalite analogues. This is due to the higher energy of S 3p with respect to O 2p atomic orbitals, which causes a separation of the cluster states from the cage states.

1. Introduction

In the past 20 years, experimental and theoretical studies of semiconductor nanoparticles have become increasingly important.[1] This is mainly because of the tunability of the electronic properties of these systems, which is useful in optoelectronics.[2] In fact, when the particle size is reduced, changes in energy associated with the electronic transitions shift toward higher values, with a concomitant concentration of the oscillator strength into just a few transitions. In the simplest approximation, this quantum size effect or quantum confinement effect can be considered as the experimental accomplishment of a particle in a box.[1−3]

Various synthetic routes have been proposed to control the particle size. Of them, we mention the passivation of the cluster surface with "capping" ligands[4−7] and the inclusion of nanoclusters in solid hosts such as glasses or zeolites.[8] With specific reference to the encapsulation of nanoparticles into zeolite cages, it is of relevance to note that this strategy allows for the creation of periodic tridimensional cluster assemblies.[8] The study of the interplay between structural and electronic properties of these systems is interesting because of the correlation existing between the structure and the fundamental gap.[4−8]

Optical and electronic properties of Cd_4S and Zn_4O clusters encapsulated in sodalite borate and aluminate cages, respectively, have been experimentally studied in the recent past.[9−11] In this regard, Blasse et al.[11] showed that the efficient luminescence of these materials is a consequence of the strong localization on the Zn_4O and Cd_4S clusters of the states involved in the optical transitions.[12]

As a part of a systematic investigation of molecular models[14] of extended systems, we studied both theoretically and experimentally the series of complexes hexakis[μ-acetate-O:O′]-μ_4-oxo-tetrazinc ([$Zn_4(\mu_4$−O){μ-O_2CCH_3}$_6$]),[5a] hexakis[μ-(*N*,*N*-diethylcarbamate-O:O′)]-μ_4-oxotetrazinc ([$Zn_4(\mu_4$−O){μ-O_2CNEt_2}$_6$]),[5b] hexakis[μ-(dimethylarsinodithioate-S:S′)]-μ_4-thioxotetrazinc ([$Zn_4(\mu_4$−S){μ-$S_2As(CH_3)_2$}$_6$]),[6b] hexakis[μ-(dimethylarsinodithioate-S:S′)]-μ_4-thioxotetracadmium ([$Cd_4(\mu_4$−S){μ-$S_2As(CH_3)_2$}$_6$]),[6b] and hexakis[μ-(O,O′-diethyldithiophosphate-S:S′)]-μ_4-thiotetrazinc ([$Zn_4(\mu_4$−S){μ-$S_2P(OC_2H_5)_2$}$_6$]).[6c] The goal was to determine whether these polynuclear clusters might be considered well-tailored molecular models of binary compounds (ZnO, ZnS, CdS) as well as of semiconductor−sodalite composites [$Zn_4O(BO_2)_6$, $Zn_4S(BO_2)_6$, $Cd_4S(AlO_2)_6$].[15] In the present contribution, we report the results of a theoretical investigation in which the electronic and geometrical properties of $Cd_4S(AlO_2)_6$, $Zn_4O(BO_2)_6$, and $Zn_4S(BO_2)_6$ are compared with those of the above-indicated polynuclear complexes.

2. Computational Details

2.1. Geometrical Structure. The general formula for members of the sodalite family is $M_8[T_{12}O_{24}]X_2$. TO_4 tetrahedra with T = Si^{4+}, Al^{3+}, Be^{2+}, B^{3+}, ... are connected by common O atoms to form the sodalite framework.[16] This structure is exclusively made up of face-sharing truncated octahedra that are confined by six four-membered rings and eight six-membered rings of interconnected tetrahedra (see Figures 1 and 2a). Different T cations can be present in a given system; in fact, a sodalite framework with only Si has never been found. Usually, part of the tetravalent Si^{4+} is replaced by other lower-charged cations (most commonly Al^{3+}) so that the framework composition becomes $[Al_6Si_6O_{24}]^{6-}$ as in the natural sodalite. Clearly, this framework requires charge compensation to maintain electroneutrality, and this is achieved by balancing the framework negative charges with a positively charged cluster fit into the narrow voids of the framework (the diameter of the sodalite cages is 6.6 Å). Incidentally, in addition to balancing the charge of the lattice, cluster cage cations M (typically Na^+,

* Authors to whom correspondence should be addressed: Maurizio Casarin, phone 39-49-8275164, Fax 39-49-8275161, E-mail maurizio.casarin@unipd.it; Chiara Maccato, phone 39-49-8275234, Fax 39-49-8275161, E-mail chiara.maccato@unipd.it.

† Università degli Studi di Padova.

‡ Centro di Studio della Stabilità e Reattività dei Composti di Coordinazione.

10.1021/jp013854u CCC: $22.00
Published on Web 02/19/2002

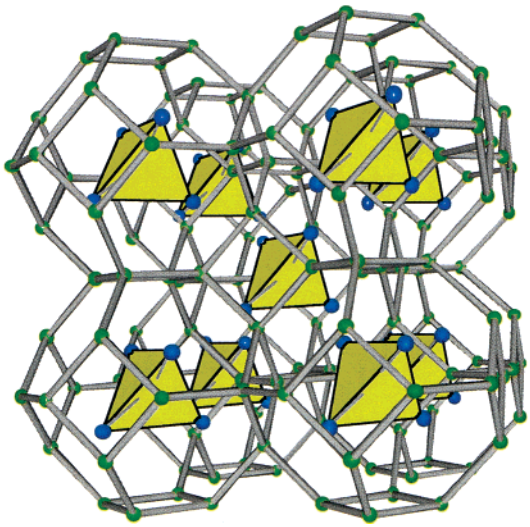

Figure 1. Schematic view of sodalite structure. The oxygen atoms have been omitted for the sake of clarity.

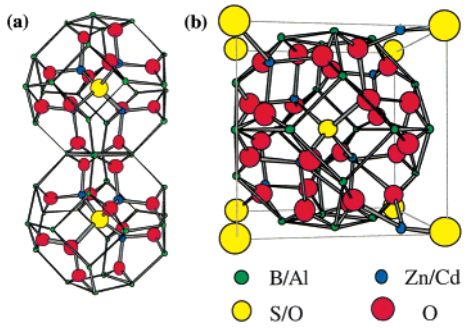

Figure 2. (a) Ball-and-stick representation of two $M_4X(YO_2)_6$ (M = Zn, Cd; X = O, S; Y = B, Al) sodalite cages. (b) Spatial arrangement of the sodalite lattice unit cell.

K^+, Ca^{2+}, ...) and cluster cage anions X (Cl^-, SO_4^{2-}, ...) prevent the opening of the sodalite framework.

Among the variety of possible sodalite compositions, we consider here three cases, $Zn_4O(BO_2)_6$, $Zn_4S(BO_2)_6$, and $Cd_4S(AlO_2)_6$. With respect to the natural sodalite, $[Al_6Si_6O_{24}](Na_4Cl)_2$, the two Zn-based sodalites are characterized by the following replacements: (i) sodium by zinc, (ii) silicon and aluminum by boron, and (iii) chlorine by oxygen/sulfur.[17−19] In these structures, all of the boron atoms are 4-fold coordinated by oxygens; furthermore, the linking of the borate tetrahedra gives rise to a tridimensional framework in which the zinc atoms are coordinated by three oxygens of the framework and by a "free" oxygen/sulfur atom, which, in turn, is bonded to four Zn atoms. Both $Zn_4O(BO_2)_6$ and $Zn_4S(BO_2)_6$ have cubic structures with lattice constants a = 7.465 6(3)[18] and 7.635(1) Å,[19] respectively, whereas the $Cd_4S(AlO_2)_6$ framework is a pure aluminate sodalite characterized by the same framework as the borate analogues [a = 8.818 1(1) Å] with boron substituted by aluminum, and zinc by cadmium. The free atom 4-fold coordinated to cadmium atoms is S.[10]

For all three considered sodalite systems, we studied the dependence of the total energy on a to find the most stable lattice geometries and their corresponding electronic properties.

2.2. Technical Details. All calculations were performed within density functional theory (DFT) using the DMol3[20,21] program, part of the Cerius2 MSI software package. Numerical wave functions obtained from solutions of the DFT equations for individual atoms were used as the basis set. Geometry optimizations were performed and binding energies were

TABLE 1: Selected Geometrical Parameters[a] of $Cd_4S(AlO_2)_6$ Relaxed Systems Calculated with Different Functionals and Compared with Experimental Data[b]

	PW91-ECP (a = exp)	PW91-ECP (a = theor)	PW91-AE (a = theor)	BP-AE (a = theor)	exp[c]
Cd−S	2.509	2.569	2.570	2.567	2.535
Cd−O	2.186	2.213	2.227	2.227	2.198
Al−O	1.761	1.773	1.767	1.768	1.749
$Cd-S_{NNN}$[d]	5.128	5.154	5.153	5.156	5.101
Cd−$\hat{S}$−Cd	109.47	109.47	109.47	109.47	−
O−$\hat{Al}$−O	107.48	107.63	107.38	107.35	108.0
Al−$\hat{O}$−A	124.61	125.55	126.31	126.17	126.1
O−$\hat{Cd}$−O	100.38	101.21	100.72	100.62	−

[a] In angstroms and degrees. [b] Theoretical results are relative to two lattice parameters: a = 8.818 Å (a = exp) and a = 8.918 Å (a = theor). [c] See ref 10. [d] NNN = next nearest neighbor.

obtained by employing the generalized gradient corrected (GGA) functional within the Perdew−Wang (PW91)[22−24] and Becke−Perdew (BP) [24,25] formulas. Double basis sets augmented by a set of d double polarization functions were adopted. Furthermore, for Zn and Cd atoms, we also used relativistic effective core potentials (ECPs) to reduce the computational cost by collecting core electrons into a single analytical representation. In this regard, we considered as core orbitals the 1s, 2s, and 2p atomic orbitals (AOs) for Zn and the 1s, 2s, 2p, 3s, 3p, and 3d AOs for Cd.[20c] ECPs give rise, because of relativistic effects, to a shortening of bond lengths (BLs).[20c] To test the importance of such effects in the present cases, we also performed nonrelativistic all-electron (AE) calculations on the three most stable geometries using both the PW91 and the BP functionals.

Numerical experiments were performed by employing the 46-atom unit cell shown in Figure 2b and limiting the k-space sampling to the Γ point. This choice, primarily dictated by the large size of the cell, is commonly adopted in similar investigations (see, e.g., ref 13). The lattice parameter a was determined by mapping the total energy onto a grid with a 0.05-Å spacing and then performing a second-order polynomial fitting. The coordinates of all 46 atoms of the unit cell were always fully optimized by using standard energy gradient techniques.

3. Results and Discussion

3.1. Cd_4S Cluster in Aluminate Sodalite Framework. The binding energy minimum corresponds to an a value of 8.918 Å (see Table 1), i.e., slightly longer than the experimental value (8.8181 Å).[10] The corresponding energy difference amounts to only 7.5 kcal/mol. Theoretical BLs and bond angles (BAs, see Table 1) agree with experiment to better than 1.5%. Furthermore, according to previous theoretical[13] and experimental[10] evidence, we found that the SCd_4 inner cluster maintains a tetrahedral symmetry. It should be noted that: (i) the calculated Cd−S BL (2.569 Å) is quite similar to the CdS bulk value (2.53 Å),[26] (ii) the equilibrium geometries are barely modified by changing the functional from PW91 to BP and by including ECPs, and (iii) the same insensitivity to exchange correlation functionals and relativistic effects holds for $Zn_4O(BO_2)_6$ and $Zn_4S(BO_2)_6$.

In Table 2, the energy difference between the highest occupied molecular orbital (HOMO) and the lowest unoccupied molecular orbital (LUMO)[27] is reported, and similarly to the equilibrium geometries, it is scarcely affected by the adopted functionals and the inclusion of relativistic corrections [all of the computed values are around 3 eV (∼400 nm)]. Furthermore, by inspecting the wave functions, we found that the HOMO and LUMO belong to the t_2 and a_1 irreducible representations, respectively, of the T_d symmetry point group. Both MOs are

TABLE 2: Electronic HOMO−LUMO Band Gaps[a] of $Cd_4S(AlO_2)_6$, $Zn_4O(BO_2)_6$, and $Zn_4S(BO_2)_6$ Calculated with Different Functionals

	PW91-ECP (a = exp)	PW91-ECP (a = theor)	PW91-AE (a = theor)	BP-AE (a = theor)
$Cd_4S(AlO_2)_6$	3.00 (413)	2.83 (438)	3.15 (394)	3.21 (386)
$Zn_4O(BO_2)_6$	3.80 (326)	3.58 (346)	3.71 (334)	3.75 (331)
$Zn_4S(BO_2)_6$	4.90 (253)	4.68 (265)	4.81 (258)	4.85 (256)

[a] In electronvolts, with values in parentheses in nanometers.

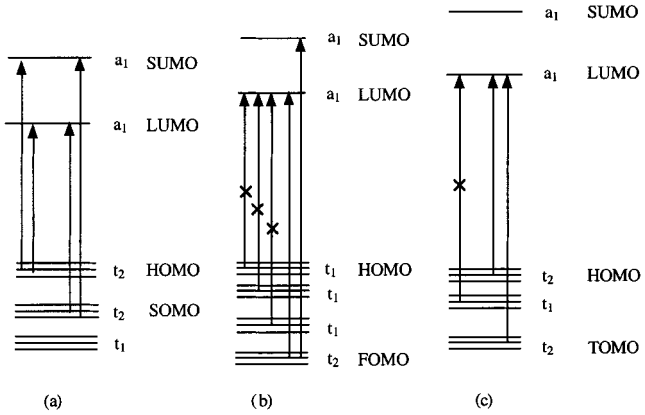

Figure 3. Qualitative outline of the frontier energy levels pertaining to (a) $Cd_4S(AlO_2)_6$, (b) $Zn_4O(BO_2)_6$, and (c) $Zn_4S(BO_2)_6$. In these schemes, all of the energy transitions are displayed, and the ones that are forbidden are marked with ×'s.

localized in the SCd_4 inner cluster though to different extents: The former includes contributions from the central sulfur (S_C) 3p AOs as well as from the 2p orbitals of the framework O atoms, whereas the latter, accounting for a S_C−Cd antibonding interaction, is almost completely localized in the SCd_4 fragment.

The HOMO (t_2) → LUMO (a_1) transition (see Table 2) is allowed by the electric dipole selection rules and reproduces very well the absorption edge at 400 nm of the UV−vis spectrum of $Cd_4S(AlO_2)_6$.[10,28] Incidentally, it is worth mentioning that this sharp absorption edge is blue-shifted by approximately 100 nm with respect to that of bulk CdS.[10] In this regard, Blasse et al.[11] also pointed out that the optical transitions of $Zn_4O(BO_2)_6$ and $Cd_4S(AlO_2)_6$ are localized in the inner cluster and that $Cd_4S(AlO_2)_6$ shows an excitation maximum at 290 nm. In Figure 3 are sketched the energy levels associated with the frontier MOs of $Cd_4S(AlO_2)_6$. Interestingly, the second unoccupied MO (SUMO) has the same a_1 symmetry as the LUMO, and the second occupied MO (SOMO) has the same t_2 symmetry of the HOMO.[30] Analogous similarities hold for the localization of the associated wave functions. On this basis, we propose the following assignments of the UV−vis spectrum of $Cd_4S(Al_6O_{12})$:[10,11] The lowest-energy absorption edge at 400 nm is due to HOMO/SOMO (t_2) → LUMO (a_1) transitions, whereas the maximum at 290 nm originates from HOMO/SOMO (t_2) → SUMO (a_1) excitations (∼260 nm, see Figure 3). In this regard, we notice some differences between our theoretical results and those of Trave et al.,[13] who reported a HOMO−LUMO gap of 2.55 eV (486 nm), with both orbitals localized on the oxygen atoms of the sodalite cage.

A few years ago, some of us synthesized and characterized, both experimentally and theoretically, a novel Cd complex ($[Cd_4(\mu_4\text{-}S)\{\mu\text{-}S_2As(CH_3)_2\}_6]$)[6b] with the aim of verifying its suitability for modeling $Cd_4S(AlO_2)_6$. The results reported herein provide further evidence that the $[Cd_4(\mu_4\text{-}S)\{\mu\text{-}S_2As(CH_3)_2\}_6]$ frontier orbitals cannot mimic the valence band top and the conduction band bottom of $Cd_4S(AlO_2)_6$. Nevertheless, it is confirmed that ligand-to-metal charge-transfer transitions of the $Cd_4(\mu_4\text{-}S)$ core reproduce very well changes in energy associated with excitations localized in Cd_4S inner clusters of $Cd_4S(AlO_2)_6$.

3.2. Zn_4O Cluster in Borate Sodalite Framework. Analogously to $Cd_4S(AlO_2)_6$, the theoretical lattice constant (a = 7.566 Å) is slightly longer (∼1%) than the experimental value (7.4659 Å, see Table 3).[18] In contrast, the differences between the theoretical and experimental BLs are larger (see Table 3) than those found for $Cd_4S(AlO_2)_6$, as far as the Zn_4O inner cluster is concerned. Finally, the HOMO−LUMO band gaps are all ∼3.7 eV (330 nm, see Table 2).

From an experimental point of view, we know that the UV spectrum of $Zn_4O(BO_2)_6$ is characterized by the presence, at 4 K, of an asymmetrical band with a maximum at 250 nm; next to this dominant band, a weaker broad band at ∼290 nm appears at room temperature.[9] At variance to the previous case, the HOMO−LUMO energy difference cannot be associated with an optical band gap. Actually, the symmetry of the HOMO is not t_2 but t_1 (see Figure 3),[31] whereas both the LUMO and SUMO have an a_1 symmetry and are both localized on the Zn_4O inner cluster (the SUMO more than the LUMO). The FOMO−LUMO and FOMO−SUMO energy differences (the lowest-energy allowed electronic transitions) are ∼4.1 eV (∼300 nm) and ∼5.1 eV (∼240 nm), respectively.[32] As a whole, these results agree quantitatively with experiment,[9,28] allowing, at the same time, a specific character to be assigned to the $Zn_4O(BO_2)_6$ optical transitions.

To our knowledge, the only proposed molecular models[14] of $Zn_4O(BO_2)_6$ are $[Zn_4(\mu_4\text{-}O)\{\mu\text{-}O_2CCH_3\}_6]$ and $[Zn_4(\mu_4\text{-}O)\{\mu\text{-}O_2CNEt_2\}_6]$.[5] The UV spectrum of the former compound shows an absorption maximum at 216 nm (5.74 eV),[33] whereas no absorption maximum has been recorded for the latter.[5b] Theoretical and experimental studies of these two complexes revealed that the lowest-lying UV transition is strongly localized on the central O atoms. Thus, on the basis of the results reported herein, we can conclude that, despite structural similarities, neither $[Zn_4(\mu_4\text{-}O)\{\mu\text{-}O_2CNEt_2\}_6]$ nor $[Zn_4(\mu_4\text{-}O)\{\mu\text{-}O_2CCH_3\}_6]$ can be considered as a molecular model of $Zn_4O(BO_2)_6$.

3.3. Zn_4S Cluster in Borate Sodalite Framework. The first thing to note about $Zn_4S(BO_2)_6$ is the lack of experimental structural information; in fact, only the a parameter (7.635 Å) is reported in the literature.[19] Once again, the theoretical a value (7.700 Å) is slightly longer than the experimental one (see Table 4). Moreover, there are only minor variations between geometrical parameters pertinent to the experimental and optimized a values (see Table 4).

Interestingly, the HOMO and LUMO symmetries (see Figure 3) are the same as were found in $Cd_4S(AlO_2)_6$. Very close in energy to the HOMO (t_2) are two other triply degenerate occupied MOs of t_1 and t_2 symmetries. The lowest-lying electronic transitions (HOMO → LUMO and TOMO → LUMO) lie at ∼4.80 eV (∼260 nm) and ∼5.05 eV (∼245 nm), respectively (see Table 2 and Figure 3). Moreover, as in the other two sodalites, these two transitions involve MOs that are almost completely localized in the inner clusters. Unfortunately, no UV absorption data are available for comparison. However, Blasse et al.[11] estimated that the excitation maximum of $Zn_4S(BO_2)_6$ should be around 230 nm, i.e., with respect to the excitation maxima of $Cd_4S(AlO_2)_6$ and $Zn_4S(BO_2)_6$, in agreement with our findings.

The comparison of the theoretical results for $Zn_4S(BO_2)_6$ with those collected[6c] for $[Zn_4(\mu_4\text{-}S)\{\mu\text{-}S_2P(OC_2H_5)_2\}_6]$ is in this case particularly interesting. Albinati et al.[6c] pointed out that (i) the slight trigonal distortion of the $Zn_4(\mu_4\text{-}S)$ core, observed at low

TABLE 3: Selected Geometrical Parameters[a] of $Zn_4O(BO_2)_6$ Relaxed Systems Calculated with Different Functionals and Compared with Experimental Data[b]

	PW91-ECP (a = exp)	PW91-ECP (a = theor)	PW91-AE (a = theor)	BP-AE (a = theor)	exp[c]
$Zn-O_c$[d]	1.967	2.015	2.015	2.015	1.982
$Zn-O_f$[e]	1.972	2.003	2.003	2.003	1.957
B−O	1.471	1.485	1.485	1.485	1.474
O_f-O_f	2.378/2.903	2.401/2.960	2.401/2.960	2.401/2.960	2.387/2.952
$Zn-\hat{O}_c-Zn$	109.47	109.47	109.47	109.47	–
$O_c-\hat{Z}n-O_f$	121.82	121.43	121.43	121.45	121.10
$O_f-\hat{B}-O_f$	107.85	107.87	107.87	107.87	108.16
$B-\hat{O}_f-B$	127.53	128.51	128.51	128.49	127.16
$O_f-\hat{Z}n-O_f$	94.76	95.28	95.28	95.26	95.75

[a] In angstroms and degrees. [b] Theoretical data reported relative to two lattice parameters: $a = 7.4659$ Å (a = exp) and $a = 7.566$ Å (a = theor). [c] See ref 18. [d] O_c = "free" oxygen atoms of the OZn_4 core. [e] O_f = oxygen atoms of the sodalite framework.

TABLE 4: Selected Geometrical Parameters[a] of $Zn_4S(BO_2)_6$ Relaxed Systems Calculated with Different Functionals[b]

	PW91-ECP (a = exp)	PW91-ECP (a = theor)	PW91-AE (a = theor)	BP-AE (a = theor)
Zn−S	2.252	2.285	2.285	2.285
Zn −O	1.971	1.992	1.992	1.991
B−O	1.476	1.487	1.487	1.487
$Zn-S_{NNN}$[c]	4.356	4.383	4.383	4.383
$Zn-\hat{S}-Zn$	109.47	109.47	109.47	109.47
$O-\hat{B}-O$	107.57	107.59	107.59	107.58
$B-\hat{O}-B$	132.05	132.57	132.56	132.55
$O-\hat{Z}n-O$	101.17	101.46	101.47	101.47

[a] In angstroms and degrees. [b] Theoretical data reported relative to two lattice parameters: $a = 7.635$ Å (a = exp) and $a = 7.700$ Å (a = theor). [c] NNN = next nearest neighbor.

temperature, disappears at 300 K; (ii) the UV spectrum is characterized by a single excitation band with a maximum at 230 nm and an onset at 260 nm; and (iii) the HOMO and LUMO are localized on the S_C 3p and Zn 4s AOs, respectively.[34] A comparison of these results with the theoretical data reported herein ultimately demonstrates that $[Zn_4(\mu_4\text{-}S)\{\mu\text{-}S_2P(OC_2H_5)_2\}_6]$ is a well-tailored molecular model[14] not only of the extended ZnS but also of the $Zn_4S(BO_2)_6$ sodalite.

4. Conclusions

In the present contribution, the geometrical and electronic structures of $Cd_4S(AlO_2)_6$, $Zn_4O(BO_2)_6$, and $Zn_4S(BO_2)_6$ have been theoretically investigated. The agreement between available X-ray diffraction data and optimized geometries is satisfactory. Theoretical results allow us to assign the lowest-lying allowed electronic transitions to excitations that are almost completely localized on the M_4X inner clusters; moreover, the experimental excitation energies are well reproduced. Throughout the investigated series, the LUMOs always have a_1 symmetry and are strongly localized in the inner clusters, whereas the HOMO symmetry and its localization are sensitive to the central atom. $Zn_4S(BO_2)_6$ and $Cd_4S(AlO_2)_6$ are more easily modeled by polynuclear complexes ($[Cd_4(\mu_4\text{-}S)\{\mu\text{-}S_2As(CH_3)_2\}_6]$ and $[Zn_4(\mu_4\text{-}S)\{\mu\text{-}S_2P(OC_2H_5)_2\}_6]$) than is $Zn_4O(BO_2)_6$ because the S 3p AOs lie at higher energies than the O 2p AOs. This causes a strong localization of the HOMO on the S central atom in both the extended and the model systems, so that the lowest-energy optical transitions are similar in character. This is not the case when only oxygen anions are present, because of the extensive mixing occurring between the cluster and cage states. Consequently, the comparison with homogeneous theoretical data for $[Cd_4(\mu_4\text{-}S)\{\mu\text{-}S_2As(CH_3)_2\}_6]$, $[Zn_4(\mu_4\text{-}O)\{\mu\text{-}O_2CCH_3\}_6]$, $[Zn_4(\mu_4\text{-}O)\{\mu\text{-}O_2CNEt_2\}_6]$, and $[Zn_4(\mu_4\text{-}S)\{\mu\text{-}S_2P(OC_2H_5)_2\}_6]$ indicates that only complexes with a central S atom can be considered reasonable molecular models of the sodalite analogues.

Acknowledgment. Calculations presented herein were all carried out on SGI Origin 2000 and SGI Origin 3800 workstations at the Consorzio Interuniversitario CINECA of Bologna. This research was financially supported by INSTM (Firenze, Italy).

References and Notes

(1) (a) Alivisatos, A. P. *J. Phys. Chem.* **1996**, *100*, 13226. (b) Alivisatos, A. P.; Barbara, P. F.; Castelman, A. W.; Chang, J.; Dixon, D. A.; Klein, M. L.; McLendon, G. L.; Miller, J. S.; Ratner, M. A.; Rossky, P. J.; Stupp, S. I.; Thompson, M. E. *Adv. Mater.* **1998**, *10*, 1297.

(2) Weller, H. *Angew. Chem.* **1993**, *105*, 43.

(3) Joswig, J. O.; Springborg, M.; Seifert G. *J. Phys. Chem. B* **2000**, *104*, 2617.

(4) (a) Dance, I. G.; Choy, A.; Scudder, M. L. *J. Am. Chem. Soc.* **1984**, *106*, 6285. (b) Zeng, D.; Hampden-Smith, M. J.; Duesler, E. N. *Inorg. Chem.* **1994**, *33*, 5376. (c) Nyman, M. D.; Hampden-Smith, M. J.; Duesler, E. N. *Inorg. Chem.* **1996**, *35*, 802. (d) Farneth, W. E.; Herron, N.; Wang, Y. *Chem. Mater.* **1992**, *4*, 916. (e) Vossmeyer, T.; Reck, G.; Katsikas, L.; Haupt, E. T. K.; Schultz, B.; Weller, H. *Science* **1995**, *267*, 1476.

(5) (a) Bertoncello, R.; Bettinelli, M.; Casarin, M.; Gulino A.; Tondello, E.; Vittadini, A. *Inorg. Chem.* **1992**, *31*, 1558. (b) Casarin, M.; Tondello, E.; Calderazzo, F.; Vittadini, A.; Bettinelli, M.; Gulino, A. *J. Chem. Soc., Faraday Trans.* **1993**, *89*, 4363.

(6) (a) Bertoncello, R.; Bettinelli, M.; Casarin, M.; Maccato, C.; Pandolfo, L.; Vittadini, A. *Inorg. Chem.* **1997**, *36*, 4707. (b) Albinati, A.; Casarin, M.; Maccato, C.; Pandolfo, L.; Vittadini, A. *Inorg. Chem.* **1999**, *38*, 1145. (c) Albinati, A.; Casarin, M.; Eisentraeger, F.; Maccato, C.; Pandolfo, L.; Vittadini, A. *J. Organomet. Chem.* **2000**, *594*, 307.

(7) (a) Bowen Katari, J. E.; Colvin, V. L.; Alivisatos, A. P. *J. Phys. Chem.* **1994**, *98*, 4189. (b) Guzelian, A.; Bowen Katari, J. E.; Banin, U.; Alivisatos, A. P.; Heath, J. R. *J. Phys. Chem.* **1996**, *100*, 7212.

(8) (a) Steigerwald, M. L.; Brus, L. E. *Annu. Rev. Mater. Sci.* **1989**, *19*, 471. (b) Brus, L. E. *J. Phys. Chem.* **1986**, *90*, 2555. (c) Wang, Y.; Herron, N. *J. Phys. Chem.* **1987**, *91*, 257. (d) Wang, Y.; Herron, N. *J. Phys. Chem.* **1988**, *92*, 4988. (e) Moran, K. L.; Harrison, W. T. A.; Kamber, I.; Gier, T. E.; Bu, X.; Herren, D.; Behrens, P.; Eckert, H.; Stucky, G. D. *Chem. Mater.* **1996**, *8*, 1930.

(9) Meijerink, A.; Blasse, G.; Glasbeek, M. *J. Phys. Condens. Matter* **1990**, *2*, 6303.

(10) Brenchley, M. E.; Weller, M. T. *Angew. Chem.* **1993**, *105*, 1726.

(11) Blasse, G.; Dirksen, G. J.; Brenchley, M. E.; Weller, M. T. *Chem. Phys. Lett.* **1995**, *234*, 177.

(12) It should be noted that, in a previous theoretical investigation of the electronic structure of $Cd_4S(AlO_2)_6$,[13] both the highest occupied molecular orbitals (HOMOs, the valence band maximum) and the lowest unoccupied MOs (LUMOs, the conduction band minimum) were found to be spatially delocalized on the oxygen atoms of the sodalite framework rather than on the inner clusters.

(13) Trave, A.; Buda, F.; Selloni, A. *J. Phys. Chem. B* **1998**, *102*, 1522.

(14) A molecular model of a solid is a molecule or ion whose stereochemistry and electronic structure reasonably mimic the structural arrangement and the nature of the valence (conduction) band top (bottom) of the solid itself.[6a]

(15) Analogously to polynuclear complexes, both MX (M = Zn, Cd; X = S, O) and semiconductor−sodalite composites are characterized by the presence of penta-atomic clusters including a central X atom tetrahedrally coordinated to four metal atoms.

(16) Depmeier, W. *Acta Crystallogr. B* **1984**, *40*, 185.

(17) Smith, P.; Garcia-Blanco, S.; Rivoir, L. *Z. Kristallogr.* **1964**, *119*, 375.

(18) Smith-Verdier, P.; Garcia-Blanco, S. *Z. Kristallogr.* **1980**, *151*, 175.

(19) Levasseur, A.; Rouby, B.; Fouassier, C. *C. R. Acad. Sci. Paris* **1973**, *277*, 421.

(20) (a) Delley, B. *J. Chem. Phys.* **1990**, *92*, 508. (b) Delley, B. *J. Chem. Phys.* **1991**, *94*, 7245. (c) Delley, B. *J. Chem. Phys.* **2000**, *113*, 7756.

(21) Delley, B. *J. Phys. Chem.* **1996**, *100*, 6107.

(22) Perdew, J. P.; Chevary, J. A.; Vosko, S. H.; Jackson, K. A.; Pederson, M. R.; Singh, D. J.; Fiolhais, C. *Phys. Rev. B* **1992**, *46*, 6671; Erratum, *Phys. Rev. B* **1993**, *48*, 4978.

(23) Perdew, J. P.; Burke, K.; Wang, Y. *Phys. Rev. B* **1996**, *54*, 16533; Erratum, *Phys. Rev. B* **1998**, *57*, 14999.

(24) Wang, Y.; Perdew, J. P. *Phys. Rev. B* **1991**, *44*, 13298.

(25) Becke, A. D. *Phys. Rev. A* **1988**, *38*, 3098.

(26) Ulrich, F.; Zachariasen, W. *Z. Kristallogr.* **1925**, *62*, 260.

(27) When limiting *k*-space sampling to the Γ point, it is common to refer to the valence band maximum and conduction band minimum in terms of the HOMO and LUMO, respectively.

(28) We are perfectly aware that DFT severely underestimates the HOMO−LUMO band gap,[29] so that the very good agreement of this quantity with experimental optical absorptions could be fortuitous. However, it has to be remarked that trends are widely believed to be quite well described by this approach.

(29) Parr, R. G.; Yang, W. *Density Functional Theory of Atoms and Molecules*; Oxford University Press: New York, 1989.

(30) The HOMO and SOMO are quasi-degenerate, whereas the energy difference between the LUMO and the SUMO is ∼2 eV.

(31) It is interesting to observe that the three highest occupied molecular orbitals are t_1 in symmetry and are all localized on the sodalite oxygen atoms (O_f). The highest occupied t_2 orbital is the fourth highest occupied MO (FOMO), and it has its largest contributions from the 2p AOs of O_c and O_f.

(32) The higher intensity of the band lying at 250 nm, compared to the band at 290 nm, is probably due to the higher localization of the SUMO on the OZn_4 inner clusters.

(33) Kunkely, H.; Vogler, A. *J. Chem. Soc., Chem. Commun.* **1990**, 1204.

(34) It should be noted that, at variance to $Zn_4S(BO_2)_6$, both the HOMO and the LUMO of the $[Zn_4(\mu_4\text{-}S)\{\mu\text{-}S_2P(OC_2H_5)_2\}_6]$ complex have t_2 symmetry.